Performance Evaluation of a Vision Based Lane Tracker Designed for Driver Assistance Systems

Joel C. McCall and Mohan M. Trivedi
Computer Vision and Robotics Research Laboratory
University of California, San Diego

Abstract— **Driver assistance systems that monitor driver intent, warn drivers of lane departures, or assist in vehicle guidance are all being actively research and even put into commercial production. It is therefore important to take a critical look at key aspects of these systems, one of which being lane position tracking. In this paper we present an analysis of lane position tracking in the context of driver support systems and examine previous research in this area. Using this analysis we present a lane tracking system designed to work well under a variety of road and environmental conditions. We examine what types of metrics are important for evaluating lane position accuracy for specific overall system objectives. A detailed quantitative evaluation of the system is presented in this paper using a variety of metrics and test conditions.**

I. Introduction

WITHIN the last few years, research into intelligent vehicles has expanded from being driven mainly by autonomous driving and autonomous robot applications to applications which work with or for the human user. Human factors research is merging with intelligent vehicle technology to create a new generation of driver assistance systems that go beyond automated control systems by attempting to work in harmony with a human operator. Lane position determination is an important component of these new applications. Systems that monitor driver intent, warn drivers of lane departures, or assist in vehicle guidance are all emerging [1]–[4]. With such a wide variety of applications it is important that we examine how lane position is detected and measure performance with relevant metrics in a variety of environmental conditions.

In this paper we will first take a critical look at the overall objectives of these types of driver assistance systems and examine how lane position detection plays a role. Next, in section II, we will take a look at previous research in this area. In section III, we will explore the development of a lane position detection system in the context of a driver assistance system. Finally, in section IV we will quantify the lane position accuracy using a number of metric relevant for driver assistance applications.

A. System Objectives

In this paper we will look at driver assistance applications of lane position detection algorithms as illustrated in figure 1. For these applications it is important to examine the role that the lane position sensors and algorithms will take in the system, and design the system accordingly. The distinguishing characteristics of these systems are:

- Lane Departure Warning Systems
  For a lane departure warning system, it is important to accurately predict the trajectory of the vehicle with respect to the lane boundary. [5]
- Driver Attention Monitoring systems
  For a driver attention monitoring system, it is important to monitor the drivers attentiveness to the lane keeping task. Measures such as the smoothness of the lane following are important for such monitoring tasks. [4]

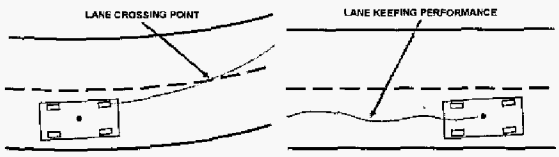

(a) lane departure warning (b) driver attention monitoring

Fig. 1. Illustrations of systems which require lane position, and key performance metrics associated with the system objectives

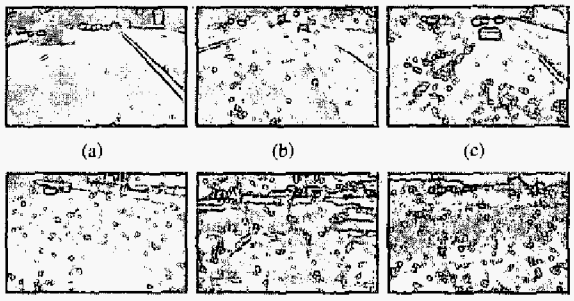

Fig. 2. Images depicting the variety of road markings for lane position determination

B. Environmental Variability

In addition to the intended application of the lane position sensing system, it is important to evaluate the type of conditions that are expected to be encountered. Road markings can vary greatly not only between regions, but also over nearby stretches of road. Roads can be marked by well-defined solid lines, segmented lines, circular reflectors (or "Botts Dots"), physical barriers, or even nothing at all. The road surface can be comprised of light or dark pavements or combinations thereof. An example of the variety of road conditions can

0-7803-8961-1/05/$20.00 ©2005 IEEE.

be seen in figure 2, all taken from roads within a mile of each other to show the variety even within a small region. In this figure, (a) shows a relatively simple scene with both solid line and dashed line lane markings. Lane position in this scene can be considered relatively easy because of the clearly defined markings and uniform road texture. Item (b) shows a more complex scene in which the road surface varies and markings consist of circular reflectors as well as solid lines. Item (c) shows a combination of circular markings and dashed line markings as well as a physical barrier. Item (d) shows a road marked solely with circular reflectors. Items (e) and (f) show complex shadowing obscuring road markings. Along with the various type of markings and road conditions, weather conditions, and time of day can have a great impact on the visibility of the road surface. This variation can be seen in figures 2e-f and 3.

Fig. 3. Images of the same stretch of road shown in the daytime and nighttime

II. Previous Work

Road and lane markings can very greatly, making the generation of a single feature extraction technique difficult. Edge based techniques can work well with solid and dashed lines, and can even be extended to attempt to compensate for circular reflectors [6]. Frequency based techniques, such as the LANA system [7], have been shown to be effective in dealing with extraneous edges. Other techniques, such as the RALPH system [8], base the lane position on an adaptive road template. These methods generally assume a constant road surface texture and can fail in situations such as in figure 2b.

Road modelling can be effective in increasing system performance by helping to eliminate false positives via outlier removal. A variety of different road modelling techniques have been used. This variety of techniques stems from the wide variety of roads. Bertozzi and Broggi [9] assumed simply that the road markings for parallel lines in an inverse perspective warped image. More recently, deformable contours such as splines have been used to parameterize roads [10].

The two most common tracking techniques used in lane position detection systems are Kalman filtering [11] and particle filtering [12]. In these systems, feature extraction and position tracking are often combined into a closed loop feedback system in which the tracked lane position defines an a priori estimate of the location and orientation of the extracted features.

III. Vision Based Lane Position Detection For Driver Assistance

Breaking down the design into the modules described in II helps to create a lane position detection system focused on one or more of the system objectives described in section I-A and capable of handling a variety of the environmental conditions explored in section I-B. By examining the system one piece at a time and understanding how that choice might affect overall system performance we can optimize our system for our application.

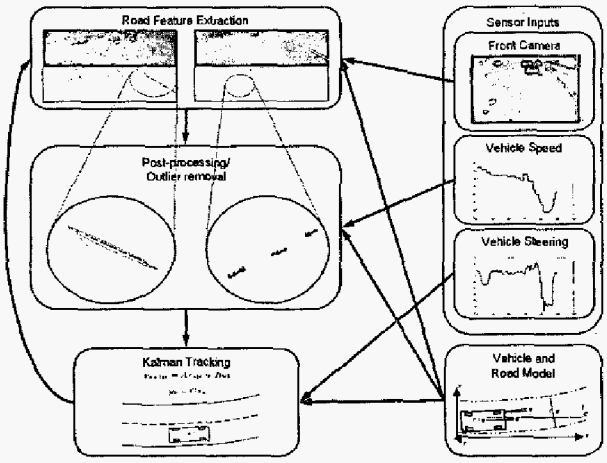

Fig. 4. System flow for driver assistance focused lane position tracking

The system described in this section is intended to provide accurate lane position over time for the purposes of driver assistance. This includes lane departure warning and driver intent inferencing. The intended environment for the lane position detection is daytime and nighttime highway driving under a variety of different roadway conditions. These road conditions include shadowing and lighting changes, road surface texture changes, and road markings consisting of circular reflectors, dashed lines, and solid lines. The overall system that we have implemented is diagramed in Figure 4.

In this section we will describe each of the system modules and the motivation behind their development. The feature extraction and overall system is based upon our previous work presented in McCall et al. [13]. In the system presented in this paper, we expand our previous work to include more robust curvature detection, improve the road model, present an analysis of the metrics used to quantify performance, and present a detailed quantitative analysis of the performance under varying environmental and road conditions.

A. Vehicle and Road Modelling

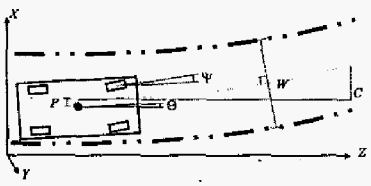

Fig. 5. Vehicle and road models used in the system

Our system objective requires a road and vehicle model that retains accuracy for distances of at least 30-40 meters. This is

required because, in critical situations in which driver assistance systems are useful, a prediction of the vehicle trajectory at least one second ahead of the vehicle is necessary. A simple parabolic road model, as shown in figure 5, incorporates position, angle and curvature while approximating a clothoid model commonly used in the construction of highway roads [11]. In the figure, X_s represents the lane offset along the center of the road, Z_s represents the distance in front of the vehicle, P represents lane position, θ represent the lane angle, C represents lane curvature, Ψ represents the steering angle, and W represents the lane width. Equation 1 describes the road down the center of the lane while equation 2 describes the road at the lane boundaries. l takes the value of 1 for the left lane and -1 for the right lane. Lane width is assumed locally constant, but is updated via a Kalman filter described in section III-E. The vehicle dynamics are approximated using a bicycle model similar to that used in Southall et al. [14]

$$X_s(Z_s) = P + \theta Z_s + C Z_s^2 \tag{1}$$

$$X_{border}(Z_s) = P + \theta Z_s + C Z_s^2 + \frac{lW}{2(\theta + C Z_s)^2 + 2} \tag{2a}$$

$$Z_{border}(Z_s) = Z_s - \frac{lW(\theta + C Z_s)}{2(\theta + C Z_s)^2 + 2} \tag{2b}$$

B. Road Feature Extraction

As previously discussed, road feature extraction is a difficult problem for a variety of reasons. For our objective and intended environment, it is necessary to have a robust estimate of road features given a variety of road marking type and conditions. Making the problem even more difficult is the necessity for fast algorithms for feature extraction. To this end, we have found features extracted by using steerable filters provide robust results for multiple types of lane markings.

$$G2^{\theta}(x,y) = G_{xx}\cos^2\theta + G_{yy}\sin^2\theta + G_{xy}\cos\theta\sin\theta \tag{3}$$

$$\theta_{min} = \arctan\left(\frac{G_{xx} - G_{yy} - A}{2G_{xy}}\right) \tag{4}$$

where

$$A = \sqrt{G_{xx}^2 - 2G_{xx}G_{yy} + G_{yy}^2 + 4G_{xy}} \tag{5}$$

G_{xx}, G_{xy}, and G_{yy} represent second derivatives of a two-dimensional gaussian.

Using the formulas 3 and 4, we can evaluate the response for a given lane angle for solid lines or find the minimum response for circular reflectors [13]. Figure 6 shows a typical highway scene with lane markings consisting of both circular reflectors and solid lines along with the image after being filtered and thresholded by the minimum response value.

These results show the usefulness of the steerable filter set for relatively normal highway conditions. This filtering technique is also very useful for dealing with shadowed regions of road. Figure 7 below shows a road section that is shadowed by trees and the filter response tuned for the lane angle.

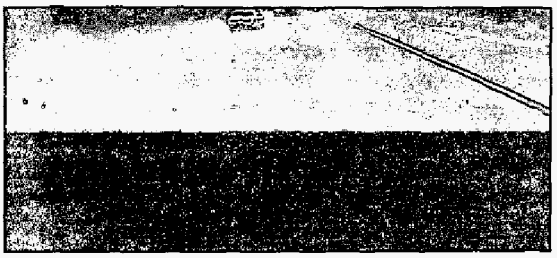

Fig. 6. Application of Steerable filter road marking recognition for circular reflectors on a highway

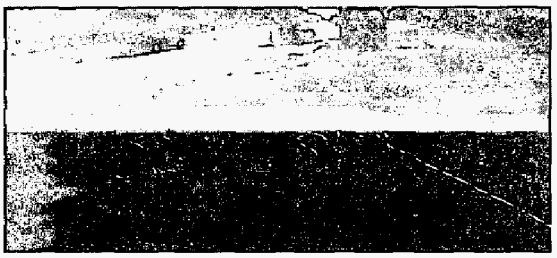

Fig. 7. Filter results when lane markings are shadowed with complex shadows and non-uniform road materials.

C. Road Curvature Estimation

Some sections of road within our intended environment are marked solely by circular reflectors as is seen in figure 2f. These circular reflectors are too small to be seen with the cameras used in our configuration at distances greater than about 20 meters. In these situations an adaptive template is used to measure curvature beyond the range of what is detectable by road markings alone. Curvature detection is performed by matching a template of the current road to the road ahead, then fitting the detected results to the lane model described in section III-A. The adaptive template is generated per pixel using a weighted average of the intensity values of the previous template and the intensity values of the lane area for the current image. The intensity values for the lane area are found by applying an inverse perspective warping to the image and cropping a rectangular area centered around the current estimate of the lane position a few meters ahead of the vehicle. The weighting can be adjusted to allow faster or slower response times and is initialized using the intensity values of the initial frame. The template is then matched to the road ahead by minimizing the squared error in intensity values of the inverse perspective warped image. The error is minimized laterally at equally-spaced distances ahead of the vehicle to get an estimate of the lateral position of the road at specific distances ahead of the vehicle. The final curvature estimate is generated by minimizing the squared error between the parabolic road model and the measured road positions.

D. Postprocessing and Outlier Removal

In order to perform robust tracking in situations such as in figures 2 and 3, some more post-processing on the filter results is performed. First, only the filter candidates within the vicinity of the lanes are used in updating the lanes. This removes

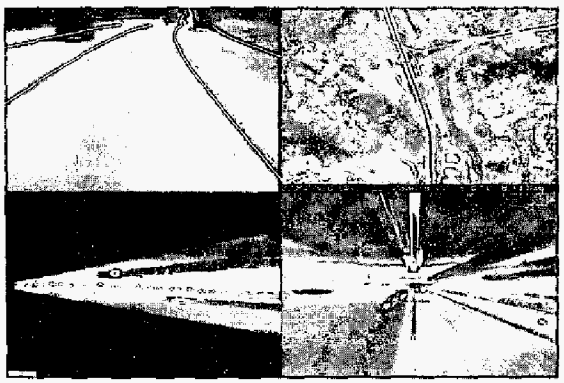

Fig. 8. Images showing curvature detection. Clockwise from upper left: Detected lanes overlaid onto image, aerial view with vehicle path highlighted, reconstructed top view from multiple cameras with lanes overlaid, inverse perspective warping showing curvature dtection and template

outliers from other vehicles and extraneous road markings. Secondly, for each lane, the first and second moments of the point candidates are computed. Straight lane markings should be aligned so that there is a high variance in the lane heading direction and a low variance in the other direction. Outliers are then removed based on these statistics. Finally, for circular reflectors, the speed of the vehicle is used to calculate the expected movement of the reflectors between half frames of an interleaved frame. This is performed using the inverse perspective equations described in 6. T and R represent the transformation and rotation of the camera respectively. The world coordinate Y is assumed zero because of the flat plane road model. Potential circular reflector detections which do not move as predicted by the ground plane are removed as outliers. Because the algorithm uses a local search about the lanes for candidates, it requires initialization. In testing, it was sufficient to initialize the lane tracker position and trajectory to zero (corresponding to the center of the lane).

$$\begin{bmatrix} x_{image} \\ y_{image} \end{bmatrix} = \begin{bmatrix} X/Z \\ Y/Z \end{bmatrix}, \begin{bmatrix} X \\ Y \\ Z \end{bmatrix} = \begin{bmatrix} R & T \end{bmatrix} \begin{bmatrix} X_{world} \\ 0 \\ Z_{world} \\ 1 \end{bmatrix} \quad (6)$$

E. Position Tracking

Position Tracking for our objective of driver assistance is vitally important. Position tracking can provide improved results in noisy situations and generate other useful metrics important for the overall system objective. Kalman filtering provides a way to incorporate a linearized version of the system dynamics to generate optimal estimates under the assumption of gaussian noise. Kalman filtering also provides estimates of state variable which are not directly observable, but may be useful for the system.

The Kalman filter state variables are updated using the lane position and angle estimates along with measurements of yaw rate (from steering angle) and wheel velocity. The lane position and angle estimates are determined using the detection statistics described in section III-D. These measurements are then used to update the discrete time Kalman filter for the road and vehicle state as described in section III-A. The system and measurement equations as well as the Kalman state equations at time step k are shown below. Road curvature ahead of the vehicle C (as apposed to the second derivative of position) is currently tracked separately.

$$x_{k+1|k} = Ax_{k|k} + Bu_k \quad (7)$$

$$y_k = Mx_k \quad (8)$$

where

$$x = [P, \dot{P} = \tan\theta, \ddot{P}, W]^T \quad (9)$$

$$A = \begin{bmatrix} 1 & v\Delta t & \frac{(v\Delta t)^2}{2} & 0 \\ 0 & 1 & v\Delta t & 0 \\ 0 & 0 & 1 & 0 \\ 0 & 0 & 0 & 1 \end{bmatrix} \quad (10)$$

$$Bu_k = [0, \Psi\Delta t, 0, 0]^T \quad (11)$$

$$M = \begin{bmatrix} 1 & 0 & 0 & 0 \\ 0 & 1 & 0 & 0 \\ 0 & 0 & 0 & 1 \end{bmatrix} \quad (12)$$

IV. Experiments and Performance Evaluation

Lane detection systems have been studied quite extensively, and several metrics for the evaluation of lane position error have been proposed [15]. However, most proposed algorithms have shown limited numerical results or have only shown selected images as results. While these images can provide information on the performance of road marking extraction in specific contexts, they fail to account for errors involved in transforming image coordinates to world coordinates and cannot be used to quantitatively compare different algorithms. In order to adequately measure the effectiveness of a lane position detection system in a specific context or system, specific metrics must be used. In this section we will explore the usefulness of a variety of performance metrics and show how the algorithm described in this paper performs based on these metrics in a variety of test conditions.

A. System Test-bed Configuration and Test Conditions

The video inputs to the system are taken from a forward looking rectilinear camera for our test results, but can be taken from any number of cameras on our test bed vehicle. For more information on this test bed, please refer to McCall et al. [16] Information about the vehicles state including wheel velocities and steering angle are acquired from the car via the internal CAN bus.

Testing was performed on highways in southern California. These highways contained road conditions shown in figures 2 and 3. Namely this includes:

- lighting changes from overpasses.
- both circular lane markers and painted line lane markers.
- shadowing from trees and vehicles.
- changes in road surface material.

A camera directed downwards at the road on the side of the vehicle provided a good view for generating hand-marked positional ground truth data. Figures 9 and 10 show results from the algorithm plotted along with the ground truth data.

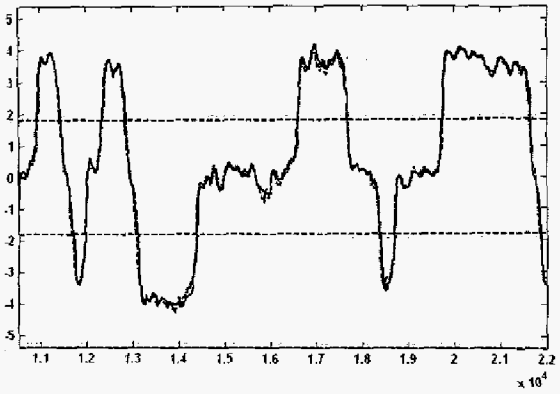

Fig. 9. Detected lane position in meters (solid blue) superimposed on ground truth (dashed red) plotted vs. frame number with dashed lines marking the position of lane boundaries for an 11,000 frame (slightly over 6 minute) sequence.

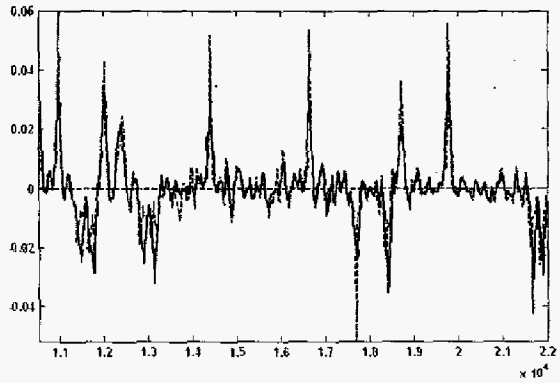

Fig. 10. Detected departure rate in m/s^2 (solid blue) superimposed on ground truth (dashed red) plotted vs. frame number with dashed line marking the abscissa for the same sequence shown in figure 9.

B. Metrics For Objective-Specific Performance Evaluation

The most common metrics for lane position performance evaluation are mean absolute error and standard deviation of error. While this provides a good estimate of the performance of a lane position tracker for system objectives such as control and driver intent, it lacks usefulness in quantifying the accuracy for other objectives. For example, road departure warning is an objective in which the rate of approach to the road boundary are important. For this reason it is important to use a variety of performance metrics when evaluating a system rather than just one.

Several metrics have been proposed to evaluate the performance of driver lane change intent and road departure warning systems. Most of these involve looking at the system as a whole and measuring false positives, false negatives, or the time it takes to trigger an alarm [1], [15], [17]. However, because the systems involve collection of data other than just lane position it is difficult to decouple the lane position performance from the system performance using these types of metrics. In order to generate an accurate prediction of performance with these objectives, it is necessary to examine the accuracy of the parameters used by the system. In this situation, we expect the metrics of error distribution of the rate of change of lane position to provide good indicators of system performance.

C. Evaluation and Quantitative Results

In order to provide a more complete test our system, we chose to quantify the error using three different metrics. The three metrics we chose are standard deviation of error (table I), mean absolute error (table II), and standard deviation of error in rate of change of lane position (table III).

Fig. 11. The 65 kilometer route used in testing overlayed on aerial photography. (photography courtesy USGS)

Results were analyzed according to these metrics under a variety of conditions as described in section IV-A. More specifically, data was collected following the roughly 65 kilometer route shown in figure 11 during both daytime and nighttime. Scenes from each of these corresponding to the points A, B, C, and D in figure 11 along with an aerial view of the individual points are shown in figure 12.

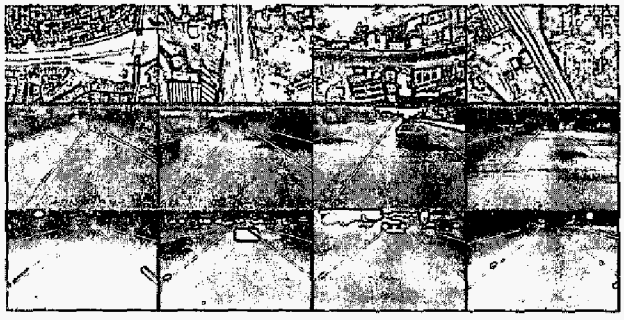

Fig. 12. Scenes from aerial views (row 1), daytime (row 2), and nighttime (row 3)

After examining the results shown in tables I, II, and III, it is interesting to note that the system actually performs

TABLE I

RESULTS FROM THE STANDARD DEVIATION OF ERROR PERFORMANCE METRIC EVALUATED UNDER VARIOUS LIGHTING AND ROAD CONDITIONS.

	Standard Deviation of Error (cm)		
Time of Day	Day	Night	Combined
Solid Lines	12.1191	9.8588	11.0193
Circular Reflectors	13.1245	10.6518	11.8130
Combined	12.6619	10.3261	**11.4714**

TABLE II

RESULTS FROM THE MEAN ABSOLUTE ERROR PERFORMANCE METRIC EVALUATED UNDER VARIOUS LIGHTING AND ROAD CONDITIONS.

	Mean Absolute Error (cm)		
Time of Day	Day	Night	Combined
Solid Lines	9.5112	6.8450	8.1503
Circular Reflectors	9.8430	8.7476	9.2352
Combined	9.6629	7.9558	**8.7616**

TABLE III

RESULTS FROM THE DEPARTURE RATE PERFORMANCE METRIC EVALUATED UNDER VARIOUS LIGHTING AND ROAD CONDITIONS.

	Standard deviation of error in departure rate metric (cm/s)		
Time of Day	Day	Night	Combined
Solid Lines	0.2716	0.2079	0.2442
Circular Reflectors	0.2808	0.2455	0.2617
Combined	0.2766	0.2304	**0.2531**

better at night. This can be attributed to the larger contrast in road markings due to their reflective nature as well as the lack of complex shadows formed by trees and vehicles during the daytime. Complex shadows hamper the systems ability to detect circular reflectors in scenes such as that shown in figure 7. Furthermore, the difference in departure rate performance between daytime and nighttime driving points to an increased number of successful detections for nighttime driving. This is likely due to the increased contrast during nighttime as the reflective road markings are illuminated by the vehicles headlamps. The comparatively smaller gain in standard deviation performance over mean absolute error might suggest that the tracking at nighttime performed better in general, but still contained cases where the tracking was off. This is because the mean absolute error metric is less influenced by the small amounts of data points that contain a larger amount of error. Also, roads that are marked with solid line markings had better results than areas marked only with circular reflectors. Again, this is most likely due to better contrast and visibility of solid line markings.

V. CONCLUSION

In conclusion, we have discussed how the overall system objective, environment, and sensor systems affect the design decisions when designing a lane position tracker. We have shown a new type of lane tracker based upon these design criteria. Finally, we have examined the metrics used to quantify accuracy of lane position systems and presented detailed quantitative results that are relevant to the systems application in a driver assistance vehicle.

Specific examples of the types of applications that this lane position tracker was designed to be used are those described in Huang et al. [18], McCall et al [4], and Gandhi et al. [?]. These systems are designed to capture the entire vehicle context including vehicle surround, vehicle state, and driver state.

ACKNOWLEDGMENT

The authors of this paper would like to thank UC Discovery Grant (Digital Media Innovations program), Nissan Motor Co. LTD., and their colleagues at the Computer Vision and Robotic Research Laboratory, especially Dr. Tarak Gandhi and Mr. Ofer Achler.

REFERENCES

[1] D. D. Salvucci, "Inferring driver intent: A case study in lane-change detection," in *Proceedings of the Human Factors Ergonomics Society 48th Annual Meeting*, 2004.

[2] W. Enkelmann, "Video-based driver assistance - from basic functions to applications," *International Journal of Computer Vision*, vol. 45, no. 3, pp. 201–221, December 2001.

[3] F. Heimes and H.-H. Nagel, "Towards active machine-vision-based driver assistance for urban areas," *International Journal of Computer Vision*, vol. 50, no. 1, pp. 5–34, 2002.

[4] J. M°Call and M. M. Trivedi, "Visual context capture and analysis for driver attention monitoring," in *Proceedings of IEEE Conference on Intelligent Transportation Systems*, October 2004, pp. 332–337.

[5] H. Godthelp, P. Milgram, and G. J. Blaauw, "The development of a time-related measure to describe driving strategy," *Human Factors*, vol. 26, pp. 257–268, 1984.

[6] Y. Otsuka, S. Muramatsu, H. Takenaga, Y. Kobayashi, and T. Monj, "Multitype lane markers recognition using local edge direction," in *Proceedings of the IEEE Intelligent Vehicles Symposium*, vol. 2, June 2002, pp. 604 – 609.

[7] C. Kreucher and S. Lakshmanan, "LANA: a lane extraction algorithm that uses frequency domain features," *IEEE Transactions on Robotics and Automation*, vol. 15, no. 2, pp. 343–350, April 1999.

[8] D. Pomerleau and T. Jochem, "Rapidly adapting machine vision for automated vehicle steering," *IEEE Expert: Special Issue on Intelligent System and their Applications*, vol. 11, no. 2, pp. 19–27, April 1996.

[9] M. Bertozzi and A. Broggi, "GOLD: a Parallel Real-Time Stereo Vision System for Generic Obstacle and Lane Detection," *IEEE Trans. on Image Processing*, vol. 7, no. 1, pp. 62–81, Jan. 1998.

[10] Y. Wang, E. Teoh, and D. Shen, "Lane detection and tracking using B-snake," *Image and Vision Computing*, vol. 22, pp. 269–280, April 2004.

[11] E. D. Dickmanns and B. D. Mysliwetz, "Recursive 3-d road and relative ego-state recognition," *IEEE Transaction on Pattern Analysis and Machine Intelligence*, vol. 14, pp. 199–213, February 1992.

[12] N. Apostoloff and A. Zelinsky, "Robust vision based lane tracking using multiple cues and particle filtering," in *Proceedings of the IEEE Intelligent Vehicles Symposium*, June 2003, pp. 558–563.

[13] J. M°Call and M. M. Trivedi, "An integrated, robust approach to lane marking detection and lane tracking," in *Proceedings of IEEE Intelligent Vehicles Symposium*, Parma, Italy, June 2004, pp. 533–537.

[14] B. Southall and C. J. Taylor, "Stochastic road shape estimation," in *International Conference on Computer Vision*, 2001, pp. 205–212.

[15] S. Szabo, K. Murphy, and M. Juberts, "The autonav / dot project: Baseline measurement system for evaluation of roadway departure warning systems," NISTIR 6300, National Institute of Standards and Technology, 1999.

[16] J. M°Call, O. Achler, and M. M. Trivedi, "Design of an instrumented vehicle testbed for developing human centered driver support system," in *Proceedings of the IEEE Intelligent Vehicles Symposium*, Parma, Italy, June 2004, pp. 483 – 488.

[17] W. Kwon and S. Lee, "Performance evaluation of decision making strategies for an embedded lane departure warning system," *Journal of Robotic Systems*, vol. 19, no. 10, pp. 499–509, 2002.

[18] K. Huang, M. M. Trivedi, and T. Gandhi, "Driver's view and vehicle surround estimation using omnidirectional video stream," in *Proceedings of IEEE Intelligent Vehicles Symposium*, Columbus, Ohio, September 2003, pp. 444–449.